Desalination and Water Treatment
www.deswater.com

doi:10.5004/dwt.2018.23059

132 (2018) 109–119
November

Graphene oxide/Mg-Fe layered double hydroxide composites for highly efficient removal of heavy metal ions from aqueous solution

Chunyan Liang, Xuezhen Feng, Jingang Yu, Xinyu Jiang*

School of Chemistry and Chemical Engineering, Central South University, Changsha 410083, China, email: lcy7089@csu.edu.cn (C. Liang), fxz867545880@csu.edu.cn (X. Feng), yujg@csu.edu.cn (J. Yu) Tel. +86-0731-88879616, email: jiangxinyu@csu.edu.cn (X. Jiang)

Received 27 January 2018; Accepted 3 September 2018

ABSTRACT

Graphene oxide/Mg-Fe layered double hydroxide (GL) composites with varying layered double hydroxide (LDH) contents were synthesized by a facile direct co-precipitation method, and then used as adsorbent to remove the heavy metal ions in aqueous solution. The structures and morphologies of GL composites were analyzed by X-ray diffraction, scanning electron microscopy, transmission electron microscopy, Fourier transform infrared spectroscopy, Raman spectra, thermal gravimetric analysis and X-ray photoelectron spectroscopy. The removal behaviors of Pb(II), Cd(II), Cu(II) and Zn(II) onto GL composites were investigated. The adsorption results could be well described by pseudo-second-order kinetic model and Langmuir model. The intraparticle diffusion model indicated that the adsorption of heavy metal ions on GL composites was a multi-step process. The thermodynamic parameters suggested that the adsorption process was spontaneous and endothermic in nature. Furthermore, the maximum adsorption capacities for Pb(II), Cd(II), Cu(II) and Zn(II) obtained from Langmuir model were about 704.23, 193.80, 229.89 and 99.21 mg g^{-1}, respectively. The as-prepared materials could effectively remove the heavy metal ions in actual wastewater.

Keywords: Graphene oxide; Layered double hydroxide; Adsorption; Heavy metal ions

1. Introduction

Heavy metal pollution have been a growing global concern due to its irreversible damage to environment and creatures [1]. Lead, copper, cadmium and zinc are typical heavy metal contaminants, which mainly released by mining, battery, metallurgy and chemical manufacturing [2]. Heavy metals in the water are bringing a great threat to human beings, animals and plants. Therefore, it is significant to dislodge the contaminants from water environment. Numerous techniques including co-precipitation, membrane filtration, solvent extraction and adsorption have been used to remove the heavy metals from wastewater [3]. Among these techniques mentioned above, adsorption has been considered the most attractive strategy for wastewater treatment due to its simplicity, high removal efficiency, feasibility and low cost. Various adsorbents such as clay minerals [4], metallic oxide [5], activated carbon and different polymers [6] have been applied to remove heavy metals from wastewater. Unfortunately, the low sorption capacity and tedious synthesis process of materials limit their practical applications. Therefore, there is a crucial demand to develop novel materials with high removal efficiency, relatively simple and economical synthesis.

Graphene oxide (GO), which is an important graphene-based nanomaterial, possess plenty of oxygen-containing functional groups such as carboxyl (–COOH), carbonyl (–C=O), epoxy(C–O–C) and hydroxyl (–OH) [7,8]. These functional groups contribute to bind metal cations through electrostatic interaction and coordination, thus they are significant for efficiently removing heavy metals from wastewater. However, it worth noting that the disadvantage of difficult segregation and easy agglomeration significantly limit the application of GO in wastewater treatment [9].

*Corresponding author.

Recently, the surface of graphene oxide has been functionalized with different nanomaterials and molecules to overcome these disadvantages and further improve the adsorption efficiency.

Layered double hydroxides (LDHs), which are also known as a category of synthetic anionic clay or hydrotalcite-like compounds (HTLC) [10], have received a lot of attention due to their unique property and relatively facile synthetic process. The structures of LDHs can be represented by the general formula $[M^{2+}_{1-x}M^{3+}_{x}(OH)_2]^{x+}[(A^{n-})_{x/n}]^{x-}\cdot mH_2O$, where M^{2+} and M^{3+} are divalent and trivalent metal ions. The value of x is the molar ratio of $M^{3+}/(M^{2+}+M^{3+})$, and A^{n-} is the interlayer anion or gallery anion, where inorganic anions, organic anions, complex anions, isopoly and heteropolyanions are included [11]. Due to its special layered nanostructure, unique exchangeable capacity and biocompatibility, the LDHs have been widely studied and developed to remove many kinds of contaminants for water remediation applications. At the present, a variety of LDHs have been applied to remove negative charge pollutants such as SeO_3^{2-}, $Cr_2O_4^{-}$, PO_4^{3-}, NO_3^{-}, fluoride and so on, while studies on LDHs applying in removing metal cations are less reported. In addition, most studies focus on the application of Al-based LDHs, which have negative reaction of possible leaching of Al at low pH values. It is also known that excessive alumina intake has proven to be one of trigger factor of Alzheimer syndrome. Therefore, the Fe-based LDHs are more appropriate for water purification. What is more, the most reported LDHs have suffered from major defect that the LDH nanosheets are inclined to pile up together and away from well-ordered and symmetrical [12]. As a result, the specific areas decrease significantly, and thus the adsorption capacity decreases obviously [13].

Combining the merits of GO and LDHs mentioned above, a novel material with high adsorption capacity was developed in this paper. We utilized the direct co-precipitation method to synthesize the composites of GO and Mg_2Fe-OH, denoted as GO/LDH (GL) composites. The as-prepared GL composites were used as excellent adsorbents to remove heavy metal ions from water.

2. Experimental

2.1. Materials

Natural flake graphite (100 mesh, purity > 99.95%) was purchased from Nantong Xianghai Carbon Product Co., Ltd. Sulfuric acid (H_2SO_4, 98%), hydrochloric acid (HCl, 37%), phosphoric acid (H_3PO_4, 85%), potassium permanganate ($KMnO_4$) and hydrogen peroxide were obtained from Sinopharm Chemical Reagent Co., Ltd. $Mg(NO_3)_2\cdot 6H_2O$ and $Fe(NO_3)_3\cdot 9H_2O$ were provided by Tianjin Kermel Chemical Reagent Co., Ltd. Metal salts including $Pb(NO_3)_2$, $Cd(NO_3)_2\cdot 4H_2O$ and $CuSO_4\cdot 5H_2O$ and $Zn(NO_3)_2\cdot 6H_2O$ were purchased from Tianjin Fuchen Chemical Reagent Factory. All the chemicals used were of analytical grade and used as received without any further treatment.

2.2. Preparation of GO

GO was synthesized by the improved Hummer's method from natural flake graphite. The graphite was oxidized in the presence of mixed acid (H_2SO_4/H_3PO_4) and $KMnO_4$. Briefly, the mixture of graphite and $KMnO_4$ was added in the 100 mL bottomed flask, and then the 9:1 mixture of concentrated H_2SO_4/H_3PO_4 was slowly added dropwise. The mixture was heated to 50°C and stirred continuously for 12 h to introduce the oxygen-containing functional groups. After cooling to room temperature, the mixture was poured onto ice cubes. The 30% H_2O_2 was added dropwise until a brilliant yellow dispersion was obtained. Then the dispersion was washed in succession with 1 mol/L HCl aqueous solution and ultra-pure water until obtained a neutral supernatant. Finally the GO was diluted with ultra-pure water and stored in a glass bottle.

2.3. Synthesis of GL composites

The GO-LDH composites were prepared through direct co-precipitation method. Firstly, the required amount of $Mg(NO_3)_2\cdot 6H_2O$ and $Fe(NO_3)_3\cdot 9H_2O$ were dissolved in water, and then GO solution (10 mL, 10 mg mL^{-1}) was added under continuous stirring. Secondly, the NaOH solution was slowly dropped into the mixed solution under vigorous stirring conditions until a final pH = 10–10.5 was reached. Finally, the mixture was thoroughly stirred for 120 min and aged for 24 h at 60°C. After cooling to room temperature, the black slurries were washed with Milli-Q water and centrifuged several times, and then the materials were dried under vacuum-freeze for 48 h. In this experiment, the composites with different content of LDH were synthesized. Among the GL composites, the Mg/Fe molar ratio was held constant at 2:1 while the amount of $Mg(NO_3)_2\cdot 6H_2O$ were 0.2 mmol, 1 mmol and 2 mmol, respectively, which were denoted as GL_1, GL_2, and GL_3, respectively. The LDH was prepared via a similar procedure in the absence of GO.

2.4. Characterization

Field emission scanning electron microscopy (SEM, MIRA3 TESCAN) and high-resolution transmission electron microscopy (HRTEM, JEOL, JEM-2100F, Japan) were used to examine the morphologies of the materials. The phase and crystal structure were analyzed by X-ray diffraction (XRD, Rigaku D/max 2550). The surface groups were determined by Fourier transform infrared (Nicolet 6700 FT-IR spectroscopy) from 400 to 4000 cm^{-1}. Raman spectroscopy was conducted with a LabRam HR 800 spectrometer. The detailed elemental compositions were performed on an X-ray photoelectron spectroscopy (XPS) system (VG ESCALab220i-XL). Thermogravimetric analysis was investigated by using a SDT Q600 V8.0 Build 95 thermal analyzer under N_2 atmosphere. The specific surface area was calculated by the N_2 adsorption-desorption isotherms.

2.5. Adsorption experiments

In order to investigate the adsorption behavior, a typical experiment was conducted by adding 5 mg GL composites to 25 mL solution containing heavy metal ions with various concentrations and then the suspensions were shaken for a certain time. After equilibrium, the supernatant was filtered through a 0.45 μm filter membrane and the concentra-

tions of heavy metal ions were analyzed by ICP-AES. The adsorption capacities of GL composites were assessed by the following equation:

$$q_e = \frac{(C_0 - C_e)}{m} \times V \quad (1)$$

where q_e (mg g^{-1}) is the amount of heavy metal ions adsorbed per gram of adsorbent, C_0 (mg L^{-1}) and C_e (mg L^{-1}) are initial and equilibrium concentration of heavy metal ions, respectively, V (L) is the volume of the solution, m (g) is the mass of the adsorbent.

3. Results and discussion

3.1. Characterization of GL composites

The XRD patterns of pristine GO, GL composites and LDH are presented in Fig. 1. In the XRD pattern of GO, the diffraction peak at around 2θ = 9.82 was attributed to the (002) pattern of GO and corresponded to an interlayer distance of 0.90 nm. Compared with the pristine graphite (0.34 nm) [14], the interlayer spacing was expanded, probably due to the introduction of oxygen-containing functional groups on the graphite sheets and the intercalation of water molecules [15]. In the XRD pattern of LDH,the main diffraction peaks at 2θ = 11.5°, 23.1°, 33.8°, 34.0°, 38.2°, 59.5°, and 60.9° could be indexed to the (003), (006), (009), (015), (018), (110) and (013) crystal planes of Mg-Fe LDH, respectively. By using the (003) peak and Bragg equation, the d-spacing of the obtained Mg-Fe LDH was calculated to be 0.77 nm, which agreed well with the reported values of Mg-Fe LDH [13,16]. For GL composites, it was worth noting that the typical diffraction peaks of LDH weren't noticed in the GL_1 composite, which might be attributed to the few content of LDH in the GL_1 composite. As expected, with the increase of the LDH content in the composite,the typical diffraction peaks of LDH appeared, which could obviously confirm the existence of LDH. However, in all XRD patterns of GL composites, the diffraction peaks of GO were hardly noticeable, suggesting that the structure of GO changed in those composites. In addition, the sharp and symmetric peaks of GL_2, GL_3 and LDH indicated the highly crystallinity of the obtained LDH in the GL composites. From the results of XRD, we could speculate that the materials have good crystallinity and the GL composites have been successfully synthesized.

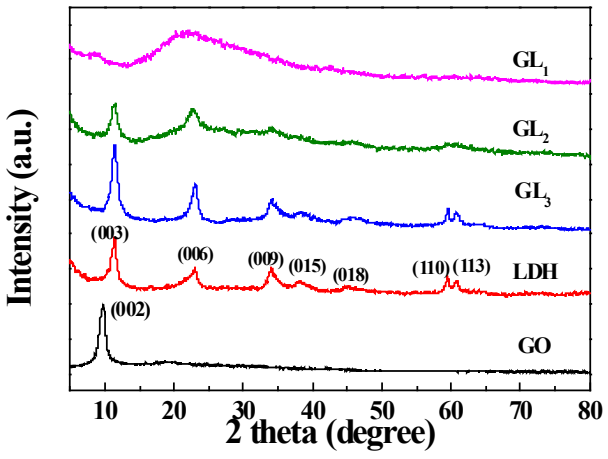

Fig. 1. XRD patterns of GO, LDH and GL composites.

The SEM and TEM micrographies of synthesized materials are depicted in Figs. 2a–e. From the SEM (Fig. 2a) and TEM (Fig. 2d) images of GO, it was seen that the GO was well-dispersed as transparent ultra thin nanosheet, which indicated graphite was successfully exfoliated into graphene oxide nanosheet. The crystal of LDH (Fig. 2b) was formed from numerous stacked-up nanoflakes, which was consistent with previous study [17]. The SEM and TEM images of GL_2 composites were presented in Fig. 2c and Fig. 2e. Compared with the smooth surface of the pure GO, numerous LDH nanosheet arrays could be observed to densely grow on the surface of GO substrate. In particular, the LDH remained firmly on the surface of GO sheet after a long period of ultrasonication process for TEM specimen preparation. This result suggested that there might be interaction between LDH and GO.

The FTIR spectra of the GL_2, LDH and GO are shown in Fig. 3. In the spectrum of GO, the O-H stretching vibration at 3403 cm^{-1}, the C=O stretching mode of the –COOH group at 1734 cm^{-1}, the C–C stretching vibration of the sp^2 carbon skeletal network at 1620 cm^{-1}, C–OH group at 1400 cm^{-1} and the alkoxy C–O group at 1114 cm^{-1} were observed. This revealed that the oxygen-containing groups were successfully introduced onto the surface of graphene. In the spectrum of the LDH sample, the broad strong band at 3440 cm^{-1} was attributed to the O–H stretching vibration in the brucite-like layers, physically adsorbed water and interlayer water. And another band corresponding to water molecule was located at 1632 cm^{-1}, which might confirm the presence of water in the interlayer space [18]. An intense peak at 1360 cm^{-1} could be ascribed to the $\upsilon_3$vibration of CO_3^{2-}, which indicated CO_3^{2-} ions were formed from atmospheric CO_2 and existed in the interlayer of LDH [10]; the bands around 571 cm^{-1} might be attributed to the stretching/bending vibration of metal-oxygen lattices such as O-Mg/Fe-O, Mg/Fe-O, and Mg/Fe-O-Mg/Fe [18,19]. In the FITR spectrum of GL_2 composites, the bands at 1621 cm^{-1} and 1380 cm^{-1} were the superposition of the peaks of GO and LDH, which were consistent with the previously report [1]. It was notably observed that the C=O and alkoxy C-O groups from GO were not observed in the spectrum of the GL_2 composites, possibly due to the participation of oxygen-containing groups of GO in binding with LDH and the slight thermal reduction of GO during the synthetic process [20]; the bands related with metal-oxygen lattices remained in the spectrum of GL_2 composite. These results indicated that the composite was successfully prepared.

In order to further investigate the structure and vibrational properties of the as-prepared materials, the Raman analysis was performed. Fig. 4 displays the Raman spectra of pure GO and GL_2 composite. The Raman spectrum was characterized by two main bands: the D band at 1359 cm^{-1} corresponding to the structural defects and disordered carbon species in the graphitic layers, and the G band at 1588 cm^{-1} arising from the first-order scattering of the E_{2g} vibrational mode and corresponding to the characteristic of sp^2 hybridized C-C bond in a two dimensional hexagonal lattice [21,22]. Furthermore, the intensity ratio of the D band and

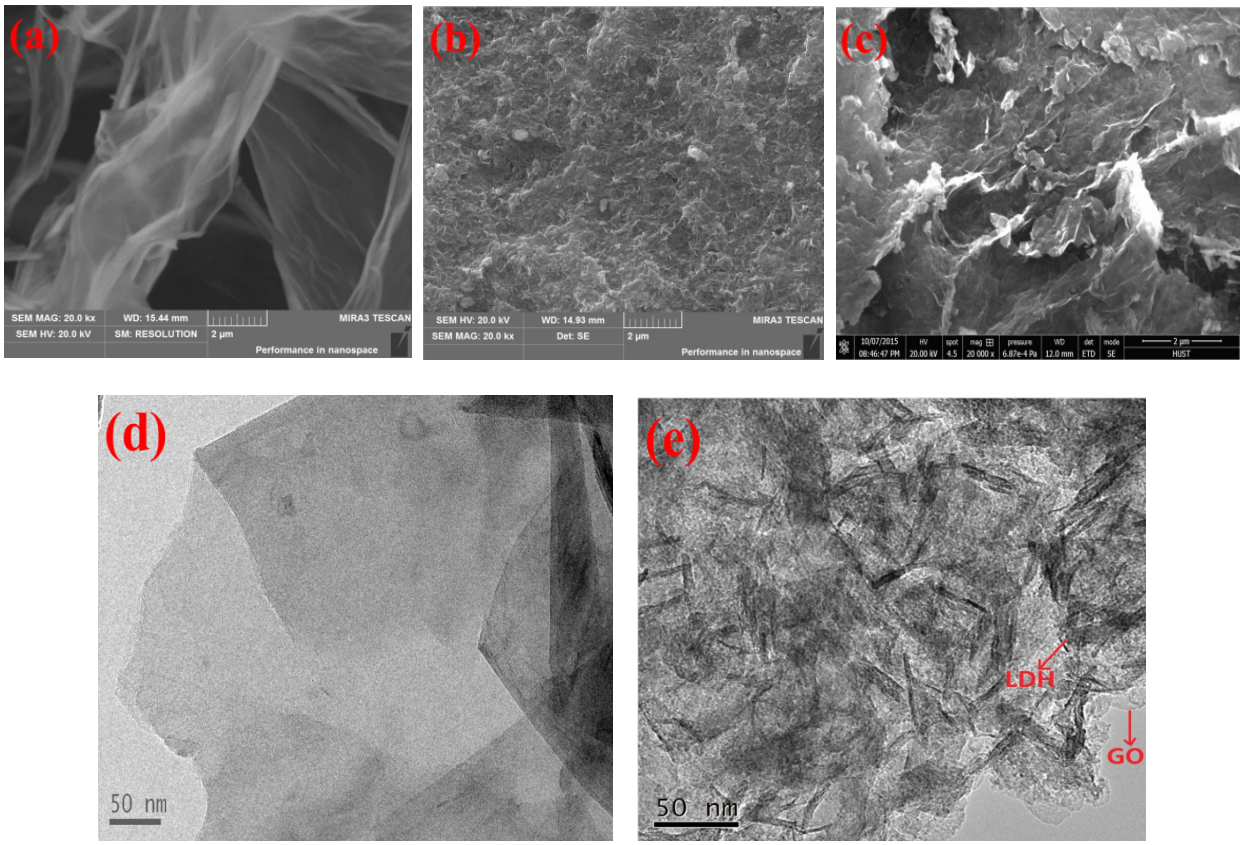

Fig. 2. SEM images of (a) GO, (b) LDH, (c) GL_2 and TEM images of (d) GO, (e) GL_2.

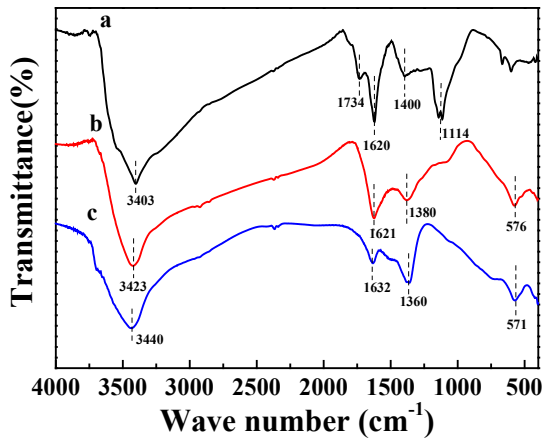

Fig. 3. FT-IR spectra of (a) GO, (b) GL_2 and (c) LDH.

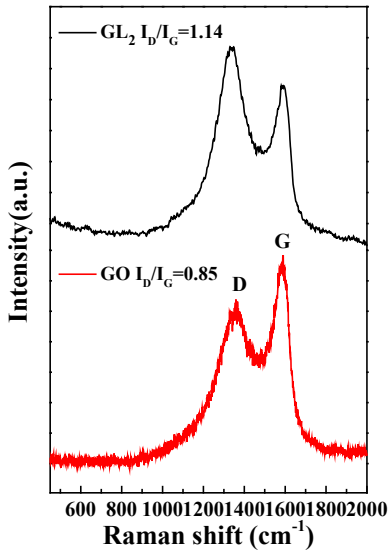

Fig. 4. Raman spectra of the as-prepared GL_2 composites and GO.

G band (I_D/I_G) represented the relatively degree of structural defects and was widely used to evaluated the disorder of graphene-based materials. As shown in Fig. 4, the value of I_D/I_G increased from 0.85 (GO) to 1.14 (GL_2), which indicated the defects on the surface of the GO increased after LDH assembly.

The thermal stability of materials was characterized by TGA curves. As shown in Fig. 5, for the pristine LDH, the weight loss process was divided into two parts. The first weight loss (about 15 wt %) from ambient temperature to 170°C was attributed to the evaporation of water physisorbed on the external surface of the crystallites and intercalated in the interlayer galleries [13]; the second weight loss (about 23 wt %) in the 170°C–700°C region presented the thermal decomposition of the hydroxyl groups in the layers and the interlayer anion [17]. For GL composites, the weight loss under below

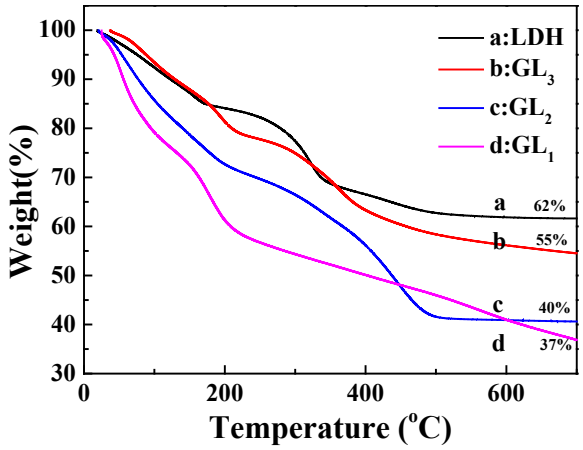

Fig. 5. The TGA curves of LDH and GL_2 composites.

200°C was ascribed to the removal of physically adsorbed water and the residual oxygen-containing functional groups on the surface of GO. The gradual weight loss above 200°C should be assigned to the main decomposition of the LDH-phase [1]. As a result, the residual weight percent of three GL composites in 700°C were 55 wt% (GL_3), 40 wt% (GL_2) and 37 wt% (GL_1), respectively. According to previous published report [1], the residue of GO was about 14 wt % in 700°C under N_2 atmosphere. Thus, the weight percentages of LDH in the GL composites were calculated to be about 85 wt % (GL_3), 54 wt % (GL_2) and 48 wt % (GL_1), respectively.

The XPS spectra of GO and GL_2 composite are given in Fig. 6. In the survey spectrum of GO, there were only two elements, named C and O. In contrast to GO, the additional Mg signal (Mg 1s, Mg KLL, Mg 2s) and Fe signal (Fe 2p) appeared in the spectrum of GL_2 composite, suggesting the existence of Mg-Fe LDH. The C1s deconvolution spectrum of GO is shown in Fig. 6b; there were four peaks positioned at 289.4, 287.9, 285.8, and 284.8 eV, which could be assigned to the carboxylate group(O-C=O), the carbonyl group (C=O) originated from carbonxylic acid, the C-O band (hydroxyl and epoxy) and aromatic linked carbon(C=C), respectively [23]. Compared with the GO, the spectrum of GL_2 also exhibited the same functionalities, while the peaks of the carbon binding to oxygen, especially the signal of C=O reduced significantly, indicating the existence of thermal reduction of GO during the prepared process [24]. It was worth noting that the binding energies (E_B) data of oxygen-containing functional groups (O-C=O, 288.2 eV; C=O, 286.4 eV; C-O, 285.3 eV) for GL_2 shifted to lower E_B values compared with those of GO, which indicated that the oxygen-containing groups on the surface of GO were involved in chemically bonding to LDH [1]. This result was agreed well with the analysis of FT-IR.

The N_2 adsorption-desorption isotherms of GO, LDH and GL_2 are shown in Fig. 7. As shown in Fig. 7, the specific surface area of GL_2 composites was calculated to be 173.86 m^2/g, which was higher than GO (28.11 m^2/g). These results proved that the addition of LDH could decrease the aggregation of graphene sheet of GO [25], resulting in an enlarged specific surface area and an improvement of the adsorption capacity of the material. Although the specific surface area of GL_2 composite was lower than that of LDH

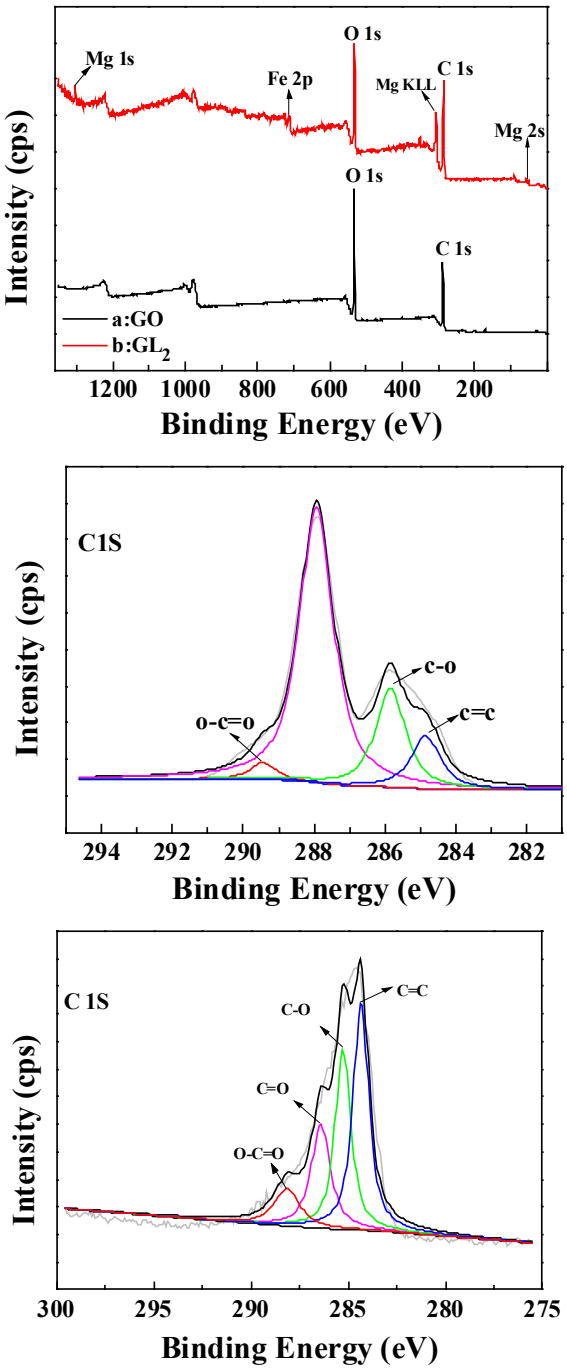

Fig. 6. (a) Survey XPS of spectra of GO (A) and GL_2 (B); (b) C 1s XPS spectra of GO; (c) C 1s XPS spectra of GL_2.

(243.30 m^2/g), GL_2 composites had higher adsorption capacity due to the introduction of abundant oxygen-containing function groups by GO composition [18].

3.2. *Removal performance of GL composites towards heavy metal ions*

Fig. 8 shows the adsorption behavior of pure GO, LDH and different GL composites tested for lead, copper,

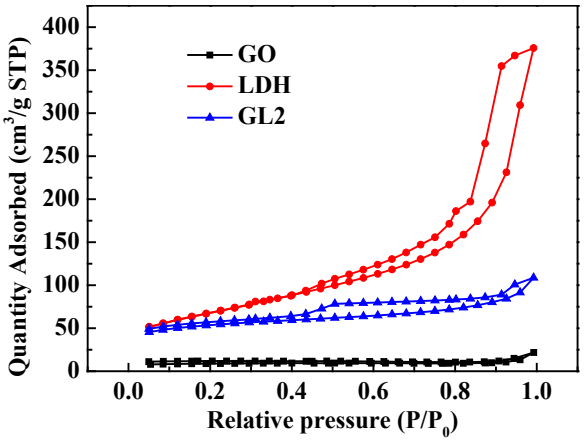

Fig. 7. N_2 adsorption-desorption isotherms of GO, GL_2 and LDH.

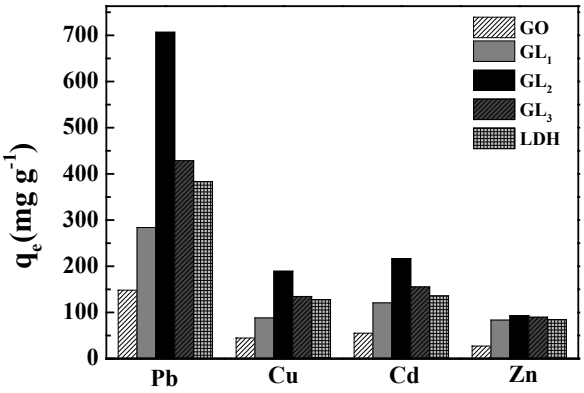

Fig. 8. The adsorption capacity of pure GO, LDH and different GL composites for Pb, Cu, Cd and Zn ions (initial concentration: 0.86 mmol/L; adsorbent: 5 mg/ 25 mL; temperature: 25°C; adsorption equilibrium: 12 h).

cadmium and zinc ions. It was found that the adsorption capacities of GL composites were evidently higher than that of pure GO, suggesting the LDH effectively reduced the restack of graphene sheet and improved the adsorption capacities. Interestingly, compared with LDH, the adsorption capacities of materials followed the sequence of GL_2 > GL_3 > LDH > GL_1. The reason for this phenomenon might be that the main component of GL_1 and GL_3 were GO and LDH, respectively, and the adsorption capacity of LDH was higher that of GO. Therefore, GL_2 composites was chosen as the adsorbent to investigate the features of adsorption process.

3.3. Adsorption kinetics

In order to analyze and study the adsorption behavior of GL composites, the kinetics of lead, copper, cadmium and zinc ions adsorption were determined. The adsorption results of Pb^{2+}, Cu^{2+}, Cd^{2+} and Zn^{2+} at different time are shown in Fig. 9a. It is seen from Fig. 9a that the necessary time to reach equilibrium is about 10 h. Therefore, 12 h was chosen for following experiment to ensure sorption equilibrium. In addition, three widely accepted kinetic model including the pseudo-first-order model [Eq. (2)], the pseudo-second-order model [Eq. (3)] and intraparticle diffusion model [Eq. (4)] were used to describe the adsorption behavior.

$$\log(q_e - q_t) = \log q_e - \frac{k_1}{2.303}t \tag{2}$$

$$\frac{t}{q_t} = \frac{1}{k_2 q_e^2} + \frac{1}{q_e}t \tag{3}$$

$$q_t = k_{di}t^{1/2} + c \tag{4}$$

where q_e (mg g^{-1}) and q_t (mg g^{-1}) refer to the adsorbed amount of heavy metal ions on the adsorbent at equilibrium time and at time t (min), respectively. k_1 (min^{-1}) and k_2 (g mg^{-1} min^{-1}) are the rate constant of pseudo-first-order and pseudo-second-order, respectively; k_{di}(mg g^{-1} $min^{-1/2}$) is the intraparticle diffusion rate constant and c is a constant related to the thickness of the boundary layer; t is the contact time.

The calculated parameters of three kinetic models are summarized in Table 1 and the fitting lines are shown in Fig. 9. As exhibited, the correlation coefficients (R^2 = 0.9972) of pseudo-second-order kinetic model were higher than those of two other models, which indicated that the adsorption process of heavy metal ions onto GL composites was mainly controlled by chemisorption involving valence forces through sharing and exchange of electrons between the adsorbents and adsorbates [26]. The intraparticle diffusion model was used to describe the diffuse process for heavy metal ions onto GL composites. The plots of q_t vs. $t^{1/2}$ were divided into three steps, indicating that the adsorption process consisted of three continuous steps: the first step was rapid external film diffusion or boundary layer diffusion, the second stage where intraparticle diffusion was rate-limiting step and the final equilibrium step for which the intrapartice diffusion started to slow down due to the lower concentration of heavy metal ions in aqueous solution [27]. In addition, the lines were not linear in the whole time range suggesting that the whole adsorption was influenced by a combination of multiple diffuse process.

3.4. Adsorption isotherms

The studies of adsorption isotherms were used to analyze the interaction between adsorbates and adsorbents, which afforded the important parameters for the determination of adsorption mechanism. The adsorption isotherms of heavy metal ions onto GL_2 composite at 25°C are depicted in Fig. 10a. As seen from Fig. 10a, the GL_2 composite exhibited a good enough adsorption capacity for heavy metal ions. The experimental results for heavy metal ions adsorption onto GL_2 composites were analyzed using Langmuir isotherm [Eq. (5)], Freundlich isotherms [Eq. (6)] and Temkin isotherms [Eq. (7)] model, and the equations are given as:

$$\frac{C_e}{q_e} = \frac{C_e}{q_m} + \frac{1}{k_L q_m} \tag{5}$$

$$\log q_e = \frac{1}{n}\log C_e + \log k_f \tag{6}$$

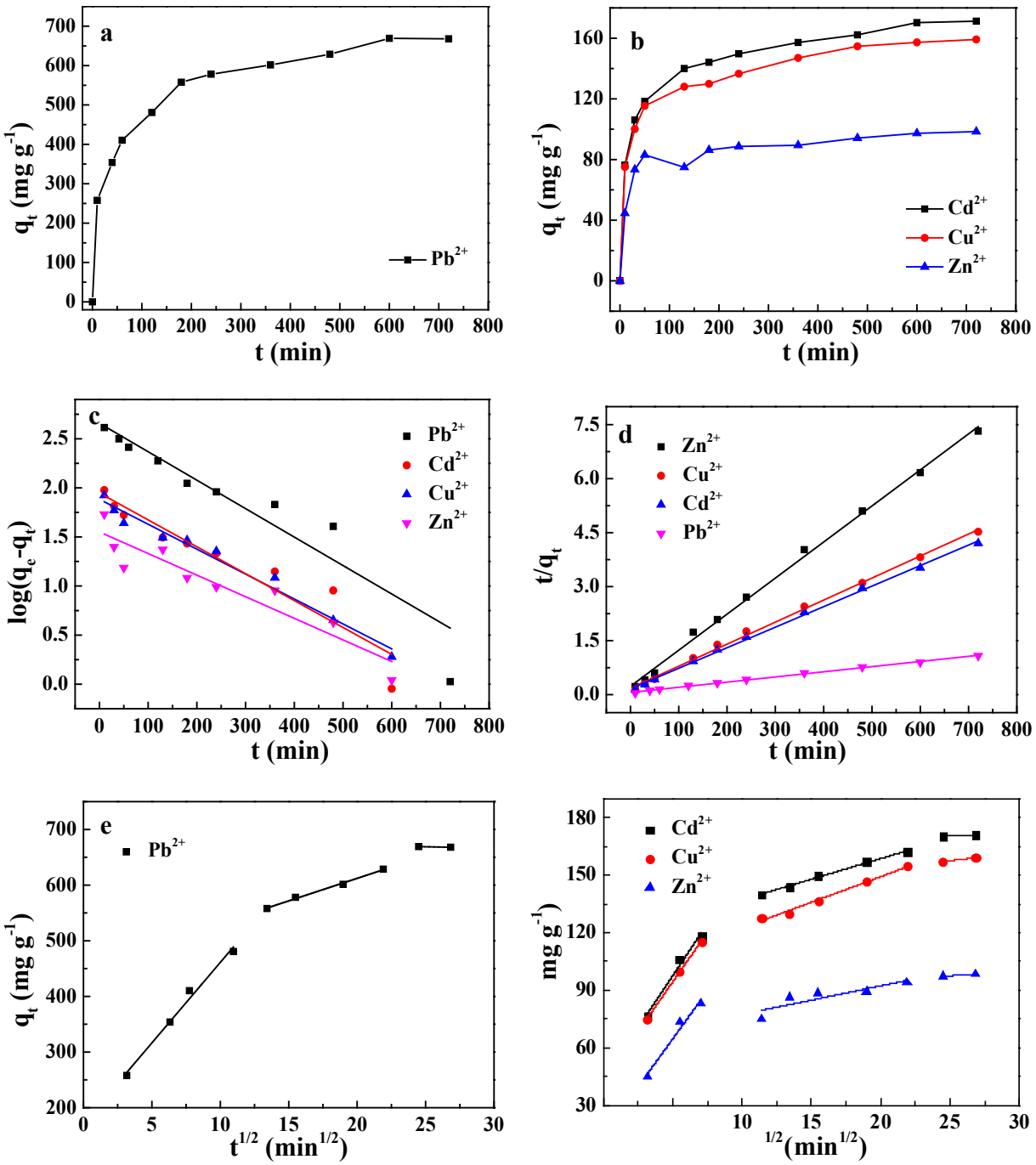

Fig. 9. (a) Effect of time on the adsorption of Pb^{2+} by GL_2 composite; (b) Effect of time on the adsorption of Cd^{2+}, Cu^{2+}, Zn^{2+} (initial concentration: 0.86 mmol/L; adsorbent: 5 mg/25 mL; temperature: 25°C); (c) pseudo-first-order kinetic model; (d) pseudo-second-order kinetic model; (e) intraparticle diffusion model for Pb^{2+} adsorption onto GL_2 composite; (f) intraparticle diffusion model for Cd^{2+}, Cu^{2+}, Zn^{2+} adsorption onto GL_2 composite.

$$q_e = \frac{RT}{b_T}\ln A_T + \frac{RT}{b_T}\ln c_e \quad (7)$$

where C_e (mg L^{-1}) is the equilibrium concentration of heavy metal ions and q_e (mg g^{-1}) is the corresponding adsorption capacity; q_m (mg g^{-1}) is the theoretical maximum Langmuir monolayer adsorption capacity, k_L is the Langmuir constant related with adsorption strength, k_f(mg/g·(mg/L)^n) and n are the constants of Freundlich isotherm indicating adsorption capacity and effectiveness, respectively. b_T and A_T are the Temkin constants related to the adsorption heat and binding energy, respectively.

The fitting plots are shown in Fig. 10b–d and the parameters are summarized in Table 2. It was found that

Table 1
Kinetic parameters for the adsorption of Pb^{2+}, Cu^{2+}, Cd^{2+} and Zn^{2+} onto GL_2 composites ([Pb^{2+}]=[Cu^{2+}]=[Cd^{2+}]=[Zn^{2+}]=0.86 mmol L^{-1})

Equations	Parameters	Pb^{2+}	Cu^{2+}	Cd^{2+}	Zn^{2+}
First-order-kinetic	q_e (mg g^{-1})	454.77	96.37	88.63	35.54
	k_1 (min^{-1})	0.0067	0.0058	0.0063	0.0051
	R^2	0.8968	0.9748	0.8878	0.8670
Second-order-kinetic	q_e (mg g^{-1})	699.30	163.39	175.44	99.90
	k_2 (g mg^{-1} min^{-1})	3.37×10^{-5}	2.15×10^{-4}	2.00×10^{-4}	4.30×10^{-4}
	R^2	0.9972	0.9972	0.9989	0.9970
Intraparticle diffusion	k_{di1} (mg g^{-1} $min^{-1/2}$)	28.93	10.36	10.91	10.024
	R^2	0.9830	0.9980	0.9669	0.9401
	k_{di2} (mg g^{-1} $min^{-1/2}$)	8.10	2.67	2.15	1.48
	R^2	0.9924	0.9820	0.9939	0.6903

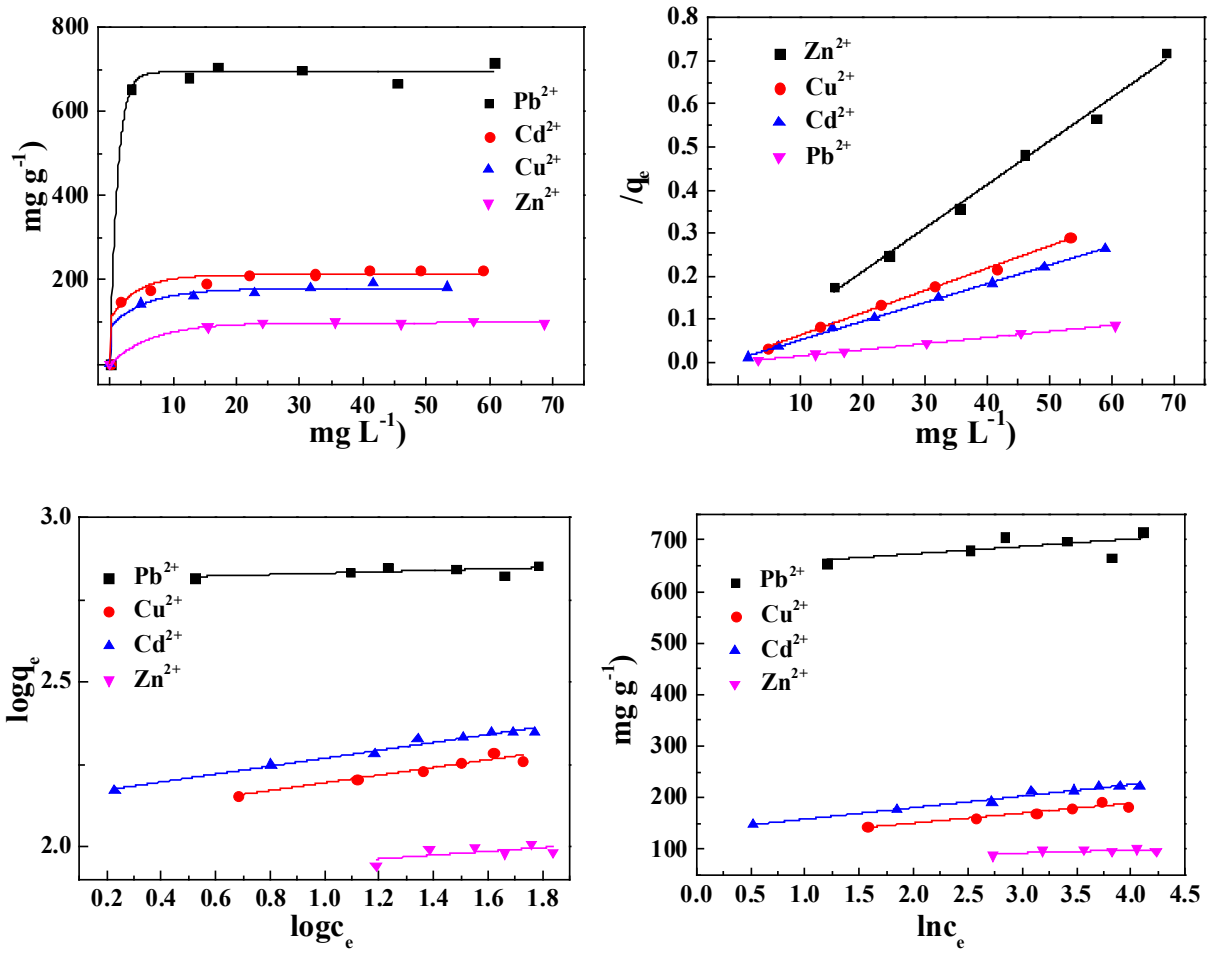

Fig. 10. (a) Adsorption isotherms of Pb^{2+}, Cu^{2+}, Cd^{2+} and Zn^{2+} onto GL_2 composite (initial concentration: 0.20–1.00 mmol/L; adsorbent: 5 mg/25 mL; temperature: 25°C; adsorption equilibrium: 12 h); (b) Langmuir isotherm; (c) Freundlich isotherm; (d) Temkin isotherm.

the regression correlations ($R^2 > 0.99$) of heavy metal ions in Langmuir isotherm model were all higher than those of other two isotherm models, therefore the Langmuir isotherm model was more suitable for describing the adsorption process. This result indicated that the monolayer adsorption played an important role in adsorption of heavy metal ions on GL_2 composites. In other word, the adsorption mainly occurred on the functional groups or binding sites on the heterogeneous surface of GL_2 composites. In addition, the maximum calculated adsorption

Table 2
Isotherm results and parameters of the adsorption of heavy metal ions onto GL_2 composites at 25°C

Isotherm	Parameter	Pb^{2+}	Cu^{2+}	Cd^{2+}	Zn^{2+}
Langmuir	q_m (mg g^{-1})	704.23	193.80	229.89	99.21
isotherm	q_m (mmol g^{-1})	3.40	3.05	2.05	1.52
	k_L	2.3854	0.4464	0.5337	1.1573
	R^2	0.9963	0.9951	0.9995	0.9935
Freundlich	n	47.35	8.56	8.31	17.41
isotherm	k_f(mg/g·(mg/L)^n)	644.83	119.31	140.53	78.21
	R^2	0.2457	0.9211	0.9726	0.2495
	A_T (L/mg)	2.59×10^{19}	430.26	442.81	1.86×10^{6}
Temkin	b_T (kJ/mol)	171.97	128.58	110.89	464.34
	R^2	0.6276	0.9608	0.9884	0.6246

amounts of Pb^{2+}, Cu^{2+}, Cd^{2+} and Zn^{2+} based on Langmuir isotherms were about 704.23 mg/g (3.40 mmol/mg), 193.80 mg/g (3.05 mmol/mg), 229.89 mg/g (2.05 mmol/g) and 99.21 mg/g (1.52 mmol/g), respectively. Obviously, the adsorption capacities followed the sequence of $Pb^{2+} > Cu^{2+} > Cd^{2+} > Zn^{2+}$.

3.5. Adsorption thermodynamic

In order to obtain more information concerning the inherent energy and define whether the process is endothermic or exothermic and spontaneous, the Pb^{2+} was chosen to investigate the thermodynamic parameters of adsorption. The effect of temperature on the adsorption of GL_2 composites for $Pb^{2+}$is shown in Fig. 11a, it can be seen that the higher adsorption capacity was obtained in higher temperature, indicating that the adsorption process was endothermic. The thermodynamic parameters (ΔH^θ, ΔS^θ, ΔG^θ) for adsorption could be calculated from the temperature dependence. The equilibrium distribution coefficient k_d and thermodynamic parameters were calculated by the following equation:

$$k_d = \frac{C_0 - C_e}{C_e} \times \frac{V}{m} \tag{8}$$

$$\ln k_d = \frac{\Delta S^\theta}{R} - \frac{\Delta H^\theta}{RT} \tag{9}$$

$$\Delta G^\theta = \Delta H^\theta - T\Delta S^\theta \tag{10}$$

where C_0, C_e, V and m are consistent with Eq. (1), R is the universal gas constant (8.314 J/mol K) and T is the absolute temperature (K). The values of ΔH^θ and ΔS^θ could be obtained from the slope and intercept of ln k_d against $1/T$ in Fig. 11b. The result is shown in Table 3. The positive values of ΔH^θ confirmed the endothermic nature of adsorption and the negative values of ΔG^θ suggested that the adsorption was spontaneous and thermodynamically favorable. Furthermore, the positive values of ΔS^θ implied an increase in degrees of freedom of the solid-solution system during the adsorption process.

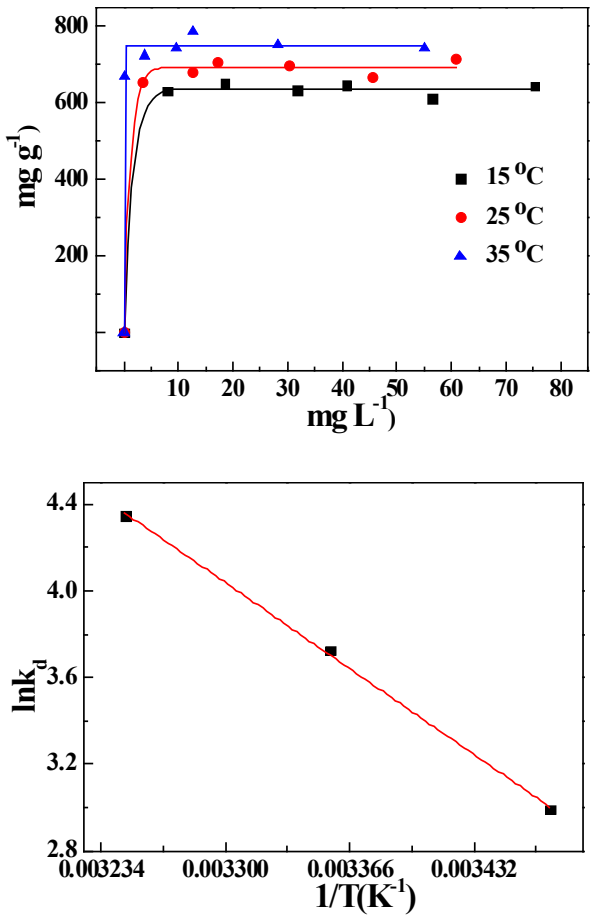

Fig. 11. (a) Effect of temperature on the Pb^{2+} uptake capacity of GL_2 composite (initial concentration: 0.20–1.00 mmol/L; adsorbent: 5 mg/25 mL; adsorption equilibrium: 12 h); (b) Plots of ln k_d versus 1/T.

3.6. Application of real sample

In order to evaluate the removal efficiency for heavy metal ions by GL_2 composites in actual wastewater, water sample was collected from a local smelter. 10 mg adsorbent

Table 3
The obtained thermodynamic parameters of Pb^{2+} adsorption onto GL_2 composites

ΔH^θ (kJ/mol)	ΔS^θ (J/K·mol)	T(K)	ΔG^θ (kJ/mol)	R^2
		288	–7.189	
49.961	198.44	298	–9.173	0.9984
		308	–11.158	

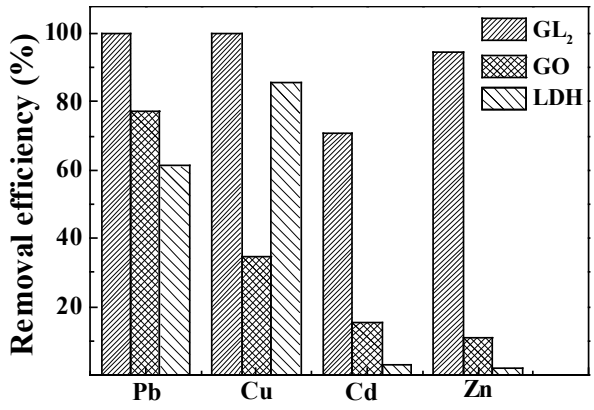

Fig. 12. The removal efficiencies of GL_2, GO and LDH for four heavy metal ions in metal smelting wastewater (adsorbent: 10 mg/20 mL; temperature: 25°C; adsorption equilibrium: 12 h).

was added into 20 mL wastewater sample, and then the mixture was shaken for 12 h. The initial concentrations of Pb^{2+}, Cu^{2+}, Cd^{2+} and Zn^{2+} in wastewater sample were 10.23 mg L^{-1}, 32.39 mg L^{-1}, 22.39 mg L^{-1} and 9.01 mg L^{-1}, respectively. The removal efficiencies of four heavy metal ions obtained from GL_2 composites, GO and LDH are presented in Fig. 12. The results showed that the removal efficiencies of four heavy metals by GL_2 composites were significantly higher than those by GO and LDH. And the removal efficiencies of Pb^{2+}, Cu^{2+}, Cd^{2+} and Zn^{2+} by GL_2 composites were 100%, 100%, 71%, and 95%, respectively. Although matrices of practical sample were complex, the GL_2 composites could effectively remove heavy metal ions in the real wastewater.

4. Conclusion

The GO/LDH composites as adsorbent for heavy metal ions were synthesized by facile direct co-precipitation method. In comparison with pure GO and LDH, the GL composites possessed higher adsorption capacity and the GL_2 composite showed the highest adsorption ability. Pseudo-second-order kinetic model and Langmuir isotherm model gave a good fit to the adsorption data, demonstrating a chemisorption and monolayer adsorption process. The positive value of ΔH^θ and negative value of ΔG^θ indicated that the adsorption was endothermic and spontaneous. The maximum adsorption capacities of Pb^{2+}, Cu^{2+}, Cd^{2+} and Zn^{2+} were 704.23, 193.80, 229.89 and 99.21 mg g^{-1}, respectively. In addition, the adsorption experiment of real wastewater showed that GL_2 composites could effectively remove the heavy metal ions in wastewater from smelter. In conclusion, GL_2 composites could be used as a promising adsorbent for removing heavy metal ions.

Acknowledgements

This work was supported by the National Natural Science Foundation of China (No. 21571191 and No. 51674292) and Provincial Natural Science Foundation of Hunan (2016JJ1023).

References

[1] F. Zhang, Y. Song, S. Song, R. Zhang, W. Hou, Synthesis of magnetite-graphene oxide-layered double hydroxide composites and applications for the removal of Pb(II) and 2,4-dichlorophenoxyacetic acid from aqueous solutions, ACS Appl. Mater. Inter., 7 (2015) 7251–7263.
[2] W. Liu, T. Wang, A.G. Borthwick, Y. Wang, X. Yin, X. Li, J. Ni, Adsorption of Pb^{2+}, Cd^{2+}, Cu^{2+} and Cr^{3+} onto titanate nanotubes: Competition and effect of inorganic ions, Sci. Total Environ., 456–457 (2013) 171–180.
[3] T. Gao, J. Yu, Y. Zhou, X. Jiang, The synthesis of graphene oxide functionalized with dithiocarbamate, J. Taiwan Inst. Chem. Eng., 71 (2017) 426–432.
[4] W. Liu, C. Zhao, S. Wang, L. Niu, Y. Wang, S. Liang, Z. Cui, Adsorption of cadmium ions from aqueous solutions using nano-montmorillonite: kinetics, isotherm and mechanism evaluations, Res. Chem. Intermediate, 44 (2018) 1441–1458.
[5] R. Ravindranath, P. Roy, A.P. Periasamy, Y.-W. Chen, C.-T. Liang, H.-T. Chang, Fe_2O_3/Al_2O_3 microboxes for efficient removal of heavy metal ions, New J. Chem., 41 (2017) 7751–7757.
[6] K. Dutta, S. De, Aromatic conjugated polymers for removal of heavy metal ions from wastewater: a short review, Environ. Sci.-Wat. Res. Technol., 3 (2017) 793–805.
[7] D.R. Dreyer, S. Park, C.W. Bielawski, R.S. Ruoff, The chemistry of graphene oxide, Chem. Soc. Rev., 39 (2010) 228–240.
[8] F. Zhou, J. Yu, X. Jiang, 3D porous graphene synthesised using different hydrothermal treatment times for the removal of lead ions from an aqueous solution, Micro Nano. Lett., 12 (2017) 308–311.
[9] S. Chowdhury, R. Balasubramanian, Recent advances in the use of graphene-family nanoadsorbents for removal of toxic pollutants from wastewater, Adv. Colloid Interface Sci., 204 (2014) 35–56.
[10] D. Zhao, G. Sheng, J. Hu, C. Chen, X. Wang, The adsorption of Pb(II) on Mg_2Al layered double hydroxide, Chem. Eng. J., 171 (2011) 167–174.
[11] X. Liang, Y. Zang, Y. Xu, X. Tan, W. Hou, L. Wang, Y. Sun, Sorption of metal cations on layered double hydroxides, Colloids Surf., A., 433 (2013) 122–131.
[12] L. Tan, Y. Wang, Q. Liu, J. Wang, X. Jing, L. Liu, J. Liu, D. Song, Enhanced adsorption of uranium (VI) using a three-dimensional layered double hydroxide/graphene hybrid material, Chem. Eng. J., 259 (2015) 752–760.
[13] M.S. Gasser, H.T. Mohsen, H.F. Aly, Humic acid adsorption onto Mg/Fe layered double hydroxide, Colloids Surf., A., 331 (2008) 195–201.
[14] S. Pourbeyram, Effective removal of heavy metals from aqueous solutions by graphene oxide–zirconium phosphate (GO–Zr-P) nanocomposite, Ind. Eng. Chem. Res., 55 (2016) 5608–5617.
[15] M. Kim, Y. Hwang, J. Kim, Graphene/MnO_2-based composites reduced via different chemical agents for supercapacitors, J. Power Sources, 239 (2013) 225–233.
[16] X. Liang, W. Hou, J. Xu, Sorption of Pb(II) on Mg-Fe layered double hydroxide, Chinese J. Chem., 27 (2009) 1981–1988.
[17] T. Wu, L. Mao, H. Wang, Adsorption of fluoride on Mg/Fe layered double hydroxides material prepared via hydrothermal process, RSC Adv., 5 (2015) 23246–23254.

[18] W. Linghu, H. Yang, Y. Sun, G. Sheng, Y. Huang, One-pot synthesis of LDH/GO composites as highly effective adsorbents for decontamination of U(VI), ACS Sustain. Chem. Eng., 5 (2017) 5608–5616.
[19] S. Yu, J. Wang, S. Song, K. Sun, J. Li, X. Wang, Z. Chen, X. Wang, One-pot synthesis of graphene oxide and Ni-Al layered double hydroxides nanocomposites for the efficient removal of U(VI) from wastewater, Sci. China Chem., 60 (2017) 415–422.
[20] Q. Fang, B. Chen, Self-assembly of graphene oxide aerogels by layered double hydroxides cross-linking and their application in water purification, J. Mater. Chem. A., 2 (2014) 8941–8951.
[21] X. Huang, M. Pan, The highly efficient adsorption of Pb(II) on graphene oxides: A process combined by batch experiments and modeling techniques, J. Mol. Liq., 215 (2016) 410–416.
[22] J. Liu, X. Ge, X. Ye, G. Wang, H. Zhang, H. Zhou, Y. Zhang, H. Zhao, 3D graphene/δ-MnO_2 aerogels for highly efficient and reversible removal of heavy metal ions, J. Mater. Chem. A., 4 (2016) 1970–1979.
[23] J. Fang, M. Li, Q. Li, W. Zhang, Q. Shou, F. Liu, X. Zhang, J. Cheng, Microwave-assisted synthesis of CoAl-layered double hydroxide/graphene oxide composite and its application in supercapacitors, Electrochim. Acta, 85 (2012) 248–255.
[24] J. Memon, J. Sun, D. Meng, W. Ouyang, M.A. Memon, Y. Huang, S. Yan, J. Geng, Synthesis of graphene/Ni–Al layered double hydroxide nanowires and their application as an electrode material for supercapacitors, J. Mater. Chem. A., 2 (2014) 5060–5067.
[25] S.P. Lonkar, J.-M. Raquez, P. Dubois, One-pot microwave-assisted synthesis of graphene/layered double hydroxide (LDH) nanohybrids, Nano-Micro Lett., 7 (2015) 332–340.
[26] Y. Ren, N. Yan, J. Feng, J. Ma, Q. Wen, N. Li, Q. Dong, Adsorption mechanism of copper and lead ions onto graphene nanosheet/δ-MnO_2, Mater. Chem. Phys., 136 (2012) 538–544.
[27] W.H. Cheung, Y.S. Szeto, G. McKay, Intraparticle diffusion processes during acid dye adsorption onto chitosan, Biotechnol. Tech., 98 (2007) 2897–2904.